Spectrometry of cosmic-ray neutrons with the High Efficiency Neutron Spectrometry Array

Álvaro Quero-Ballesteros
University of Granada & IFIC-CSIC, Valencia
alvarojquero21@ugr.es
Co-Authors: A. Tarifeño-Saldivia, N. Mont

HENSA
High Efficiency Neutron Spectrometry Array
http://www.hensaproject.org

UNIVERSIDAD DE GRANADA
IFIC INSTITUT DE FÍSICA CORPUSCULAR
CSIC CONSEJO SUPERIOR DE INVESTIGACIONES CIENTÍFICAS
UNIVERSITAT POLITÈCNICA DE CATALUNYA BARCELONATECH

The HENSA collaboration

IFIC — Institut de Física Corpuscular

CSIC — Consejo Superior de Investigaciones Científicas

Universidad de Granada

Vniversitat de València

Universitat Politècnica de Catalunya BarcelonaTech — Institut de Tècniques Energètiques

LSC — Laboratorio Subterráneo de Canfranc

TRIUMF

Universidad Zaragoza 1542

HZDR — Helmholtz Zentrum Dresden Rossendorf

Universidad Complutense Madrid

Gobierno de España — Ministerio de Ciencia e Innovación — Ciemat — Centro de Investigaciones Energéticas, Medioambientales y Tecnológicas

The origin of cosmic-ray neutrons

- Primary cosmic-rays are mainly composed of protons & He nuclei.
- Neutrons are produced as secondary particles in Extensive Air Showers (minimum energy ~500 MeV).
- Sources: SEP, Galactic & extra-galactic cosmic-rays.

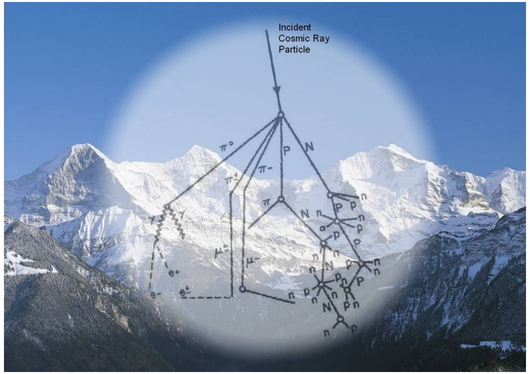

Schema: Simpson et al. (1953, Phys. Review 90, 934)

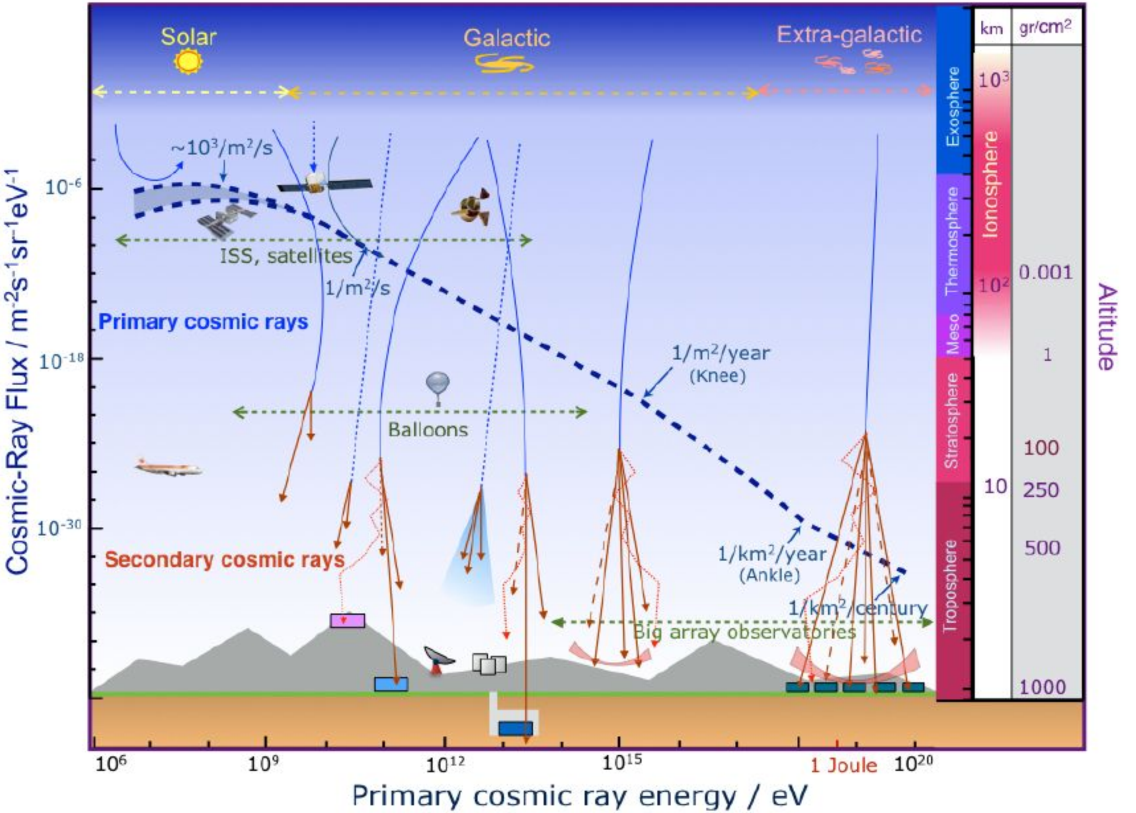

Credits Tragaldabas Collaboration

The anti-correlation between neutron flux and solar activity

Solar activity induces a modulation in the flux of galactic cosmic-rays

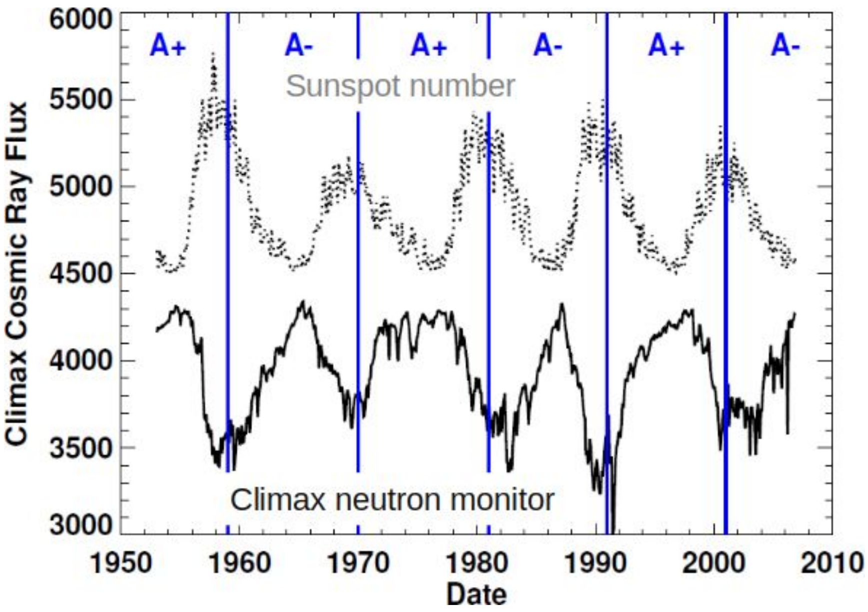

Neutron background anti-correlation with solar cycle. Cosmic Ray flux from the Climax Neutron Monitor and rescaled Sunspot Number.

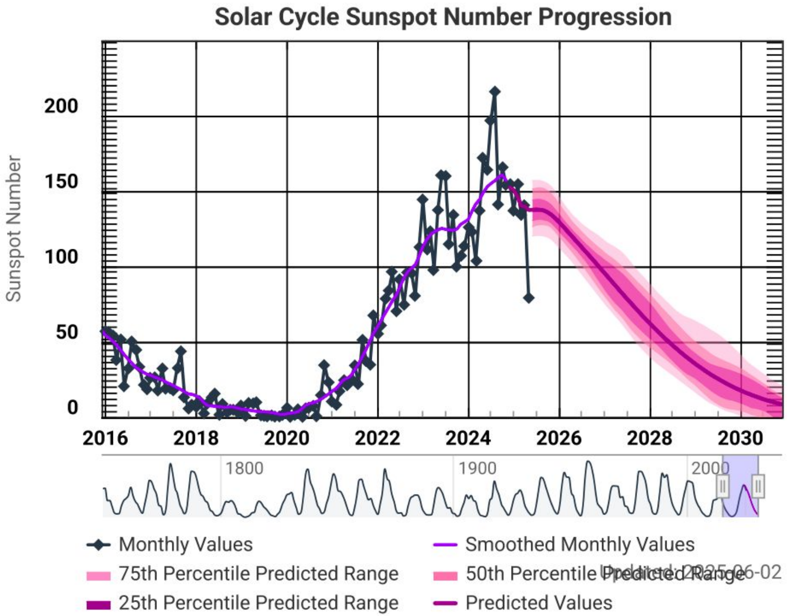

NOAA/NASA forecast for Solar Cycle 25. Updated on 30/06/2025.

Instrumentation networks on Earth for secondary cosmic-rays

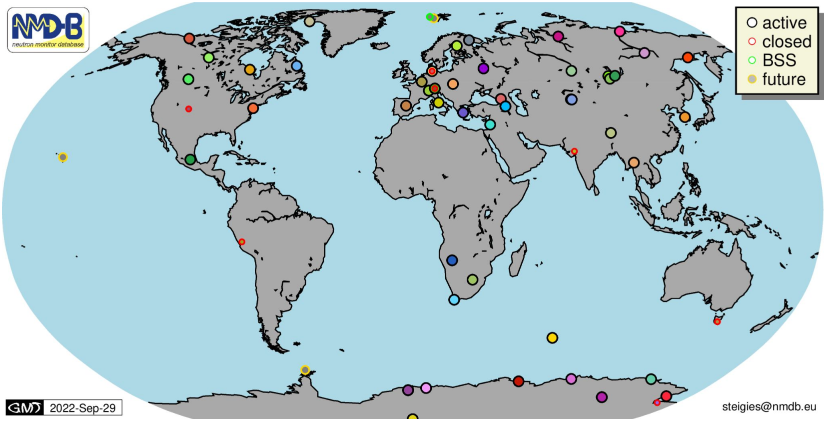

- Examples of ground-based detectors can be **neutron monitors** or **muon detectors**.

- The Neutron Monitor Database (**NMDB**) offers real-time global data from multiple neutron monitor stations, but these detectors **lack spectral resolution**.

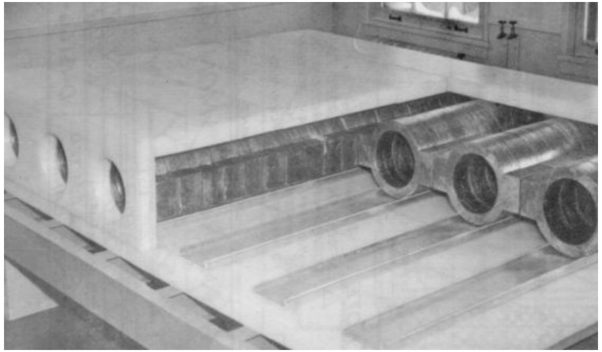

Standard neutron monitor (NM64): BF3 Tube + Polyethylene + Pb Layers

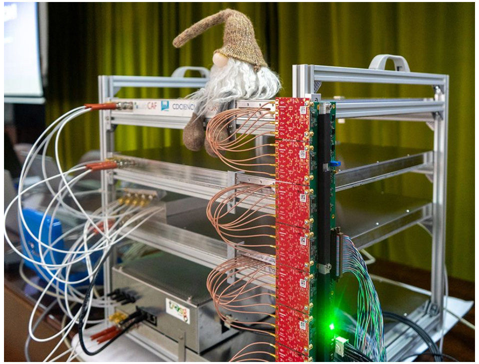

MiniTrasgo muon detector. IGFAE, Tragaldabas collaboration

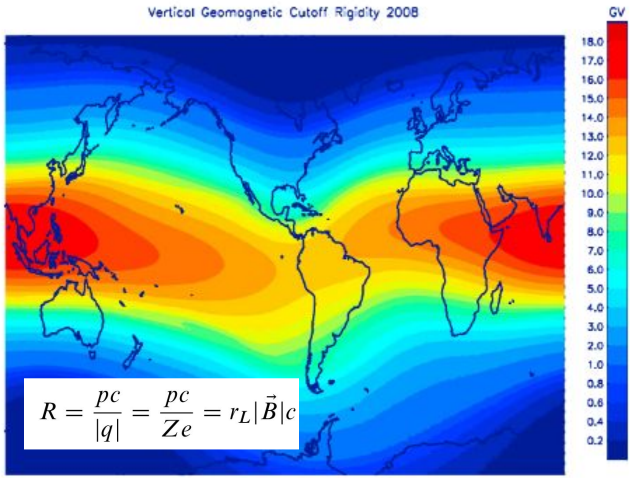

$$R = \frac{pc}{|q|} = \frac{pc}{Ze} = r_L|\vec{B}|c$$

The effect of solar events on secondary cosmic-ray radiation

Forbush Decrease (FD)

The Sun's magnetic activity temporarily reduce galactic cosmic ray flux at Earth

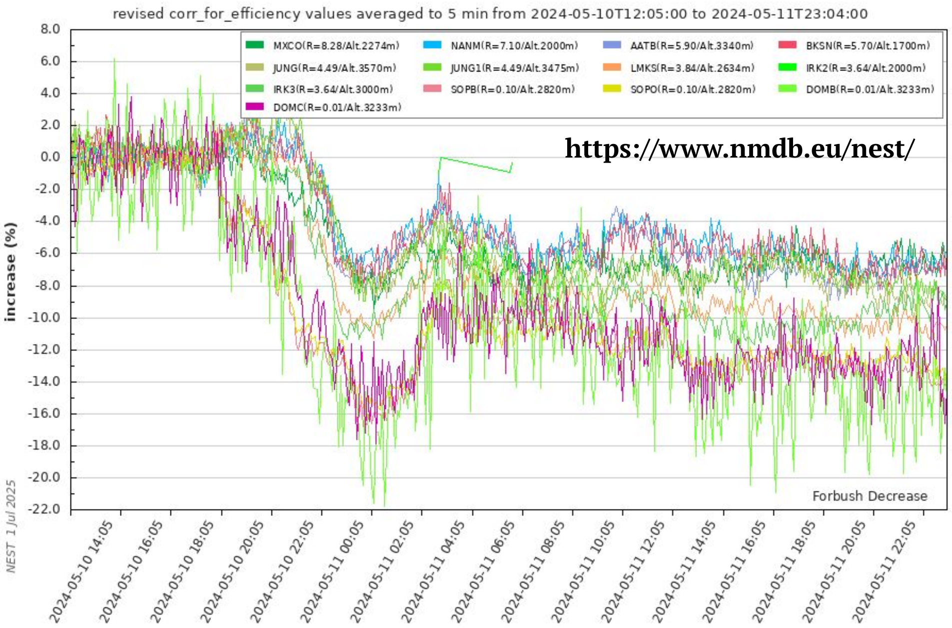

Ground Level Enhancement (GLE)

High energy solar particle events produce a temporary spike in cosmic ray intensity on Earth

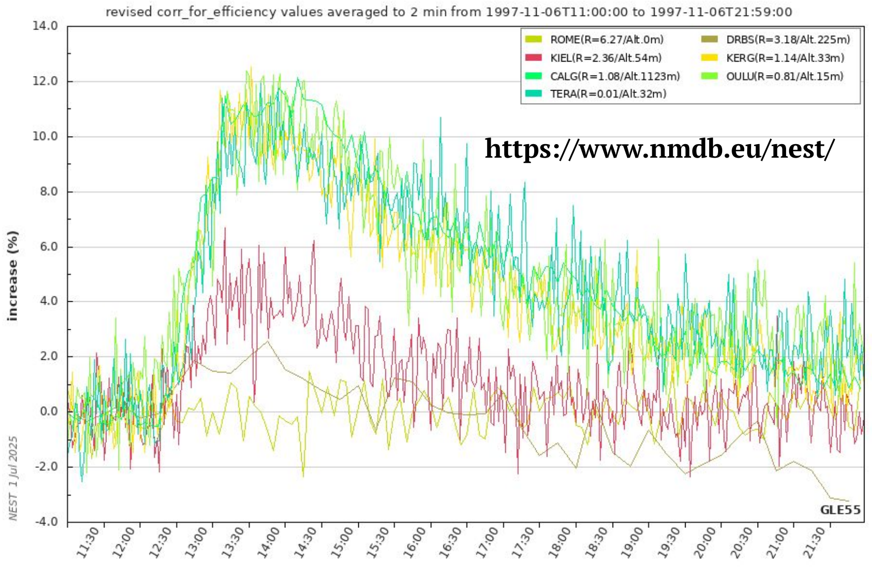

Why is it important to characterize the cosmic neutron spectrum?

We aim to **characterize the secondary cosmic-ray neutron spectrum along the solar cycle and during intense solar** storms for:

Modeling of the neutron spectrum

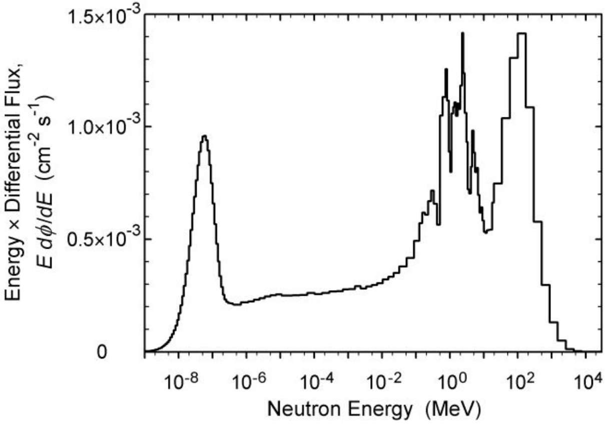

M.S. Gordon et al., IEEE Trans. Nucl. Sci. 51(6), 3427-3434 (2004).

Determination of the neutron ambient dose

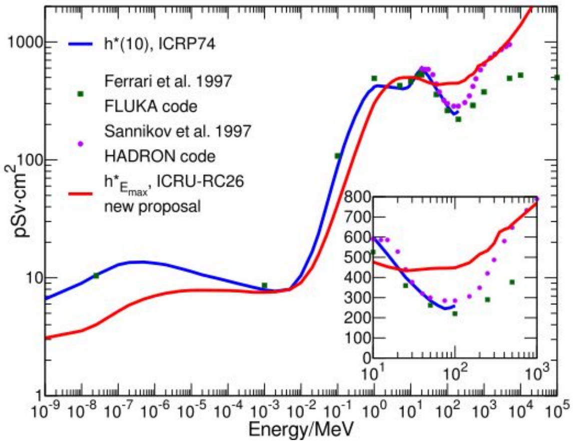

Neutron to dose conversion coefficients

Analysis of Single Events in Microelectronics

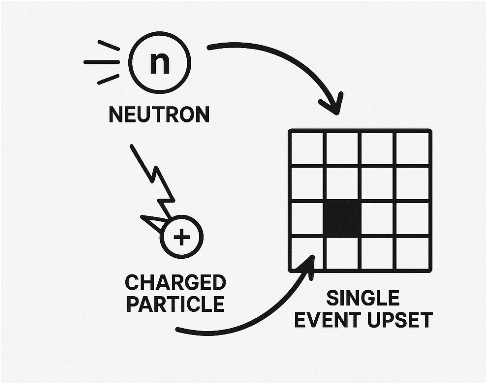

Schema of a Single Event Upset (SEU) produced by a neutron

How do we perform neutron spectrometry?

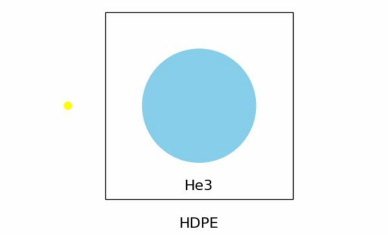

- **Detection principle** (Bonner Sphere Spectrometers):

Counter with high sensitivity to thermal neutrons + Materials with a good moderation-capture ratio and metal converters → Sensitivity from thermal to GeV neutrons

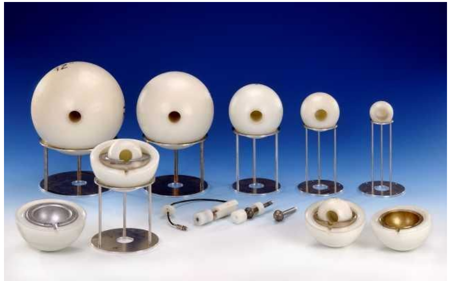

NEMUS Bonner Spheres System

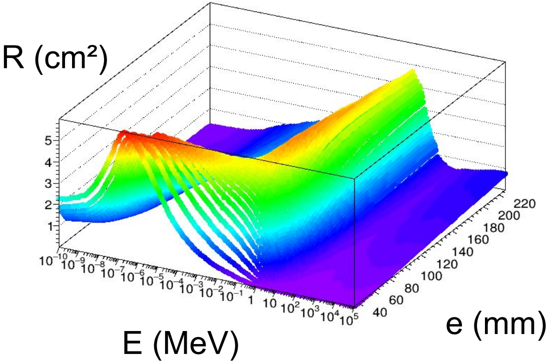

- **Spectrum reconstruction**:

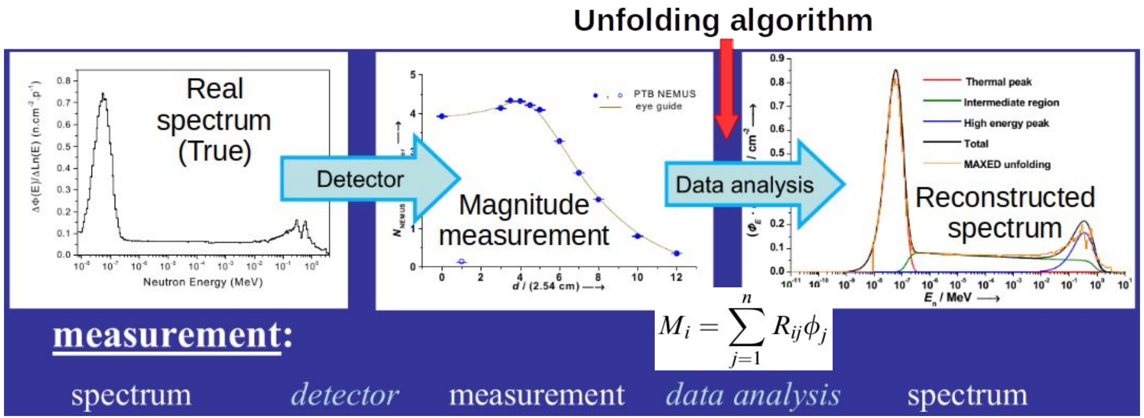

The HENSA project

http://www.hensaproject.org

HENSA
High Efficiency Neutron Spectrometry Array

- Development and application of high-efficiency neutron spectrometers
- Based on Bonner Sphere Spectrometers (BSS).
- Topology modification to increase detection efficiency (5% - 15%). Typical BSS doesn't have enough efficiency to resolve the neutron spectrum within short time intervals.
- Energy sensitivity from meV to GeV neutrons, complementing the information of NMDB.
- Main applications: Space weather, cosmic-ray physics, ambient dosimetry, underground.

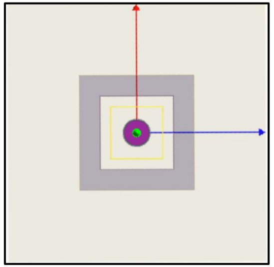

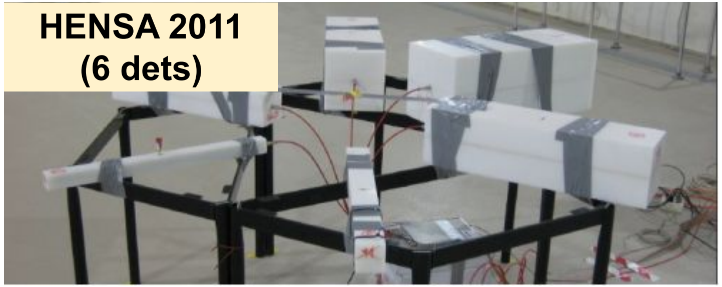

First version of HENSA (2011)

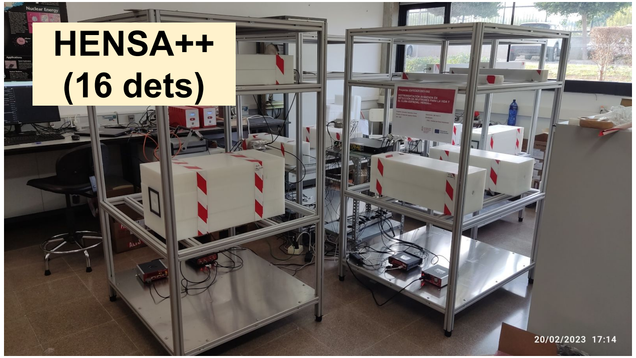

The HENSA++ spectrometer (2024)

The HENSA 2020 Cosmic-Ray Neutron Campaign

HENSA
High Efficiency Neutron Spectrometry Array

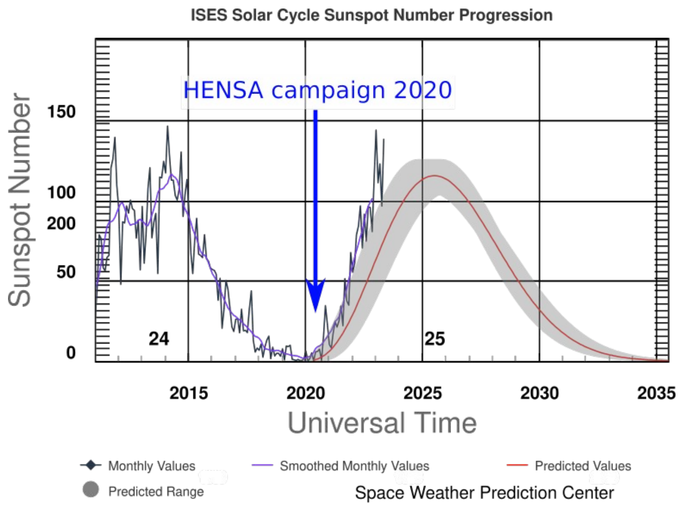

Solar activity on the HENSA 2020 campaign

HENSA campaign along the Spanish territory close to the minimum of solar activity (2020, solar cycle #25)

Cosmic ray induced neutron background
+ Cosmic ray physics and space weather
+ Environmental radiation dosimetry
+ Single-event upsets in microelectronics

HENSA
High Efficiency Neutron Spectrometry Array

www.hensaproject.org

N. Mont (PhD)

- Characterization of the cosmic-ray neutron spectrum on Rc [5.5, 8.5] GV during the minimum solar activity of cycle 25.
- Complements the range [2.5, 4.5] GV measured by Gordon et al (2004), IEEE 51(6).

Preliminary results 2020 campaign

HENSA
High Efficiency Neutron Spectrometry Array

Global Analysis

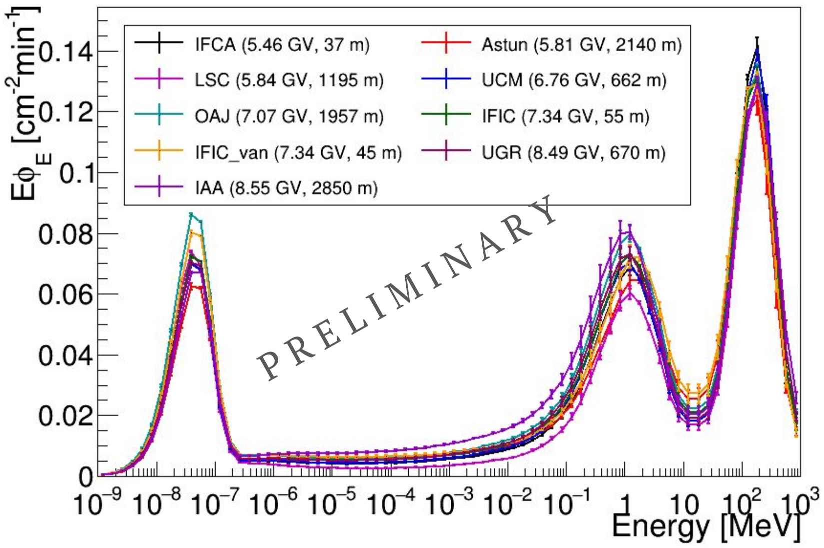

Measured neutron spectrum with HENSA, scaled by altitud and Rc in different locations

Temporal Analysis

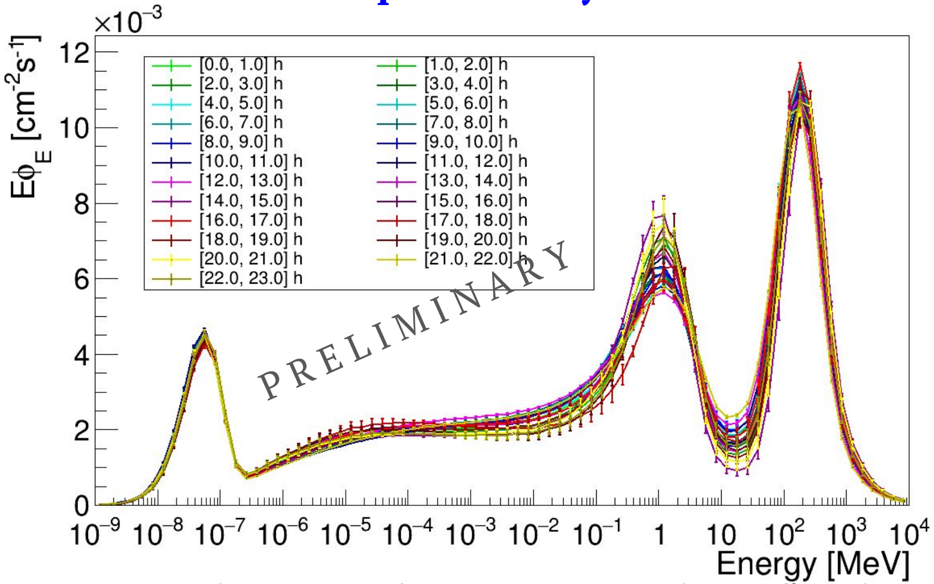

Measured spectrum with HENSA at Instituto de Astrofísica de Andalucía in time intervals of 1 hour.

- ❖ We can provide a general form for the cosmic neutron spectrum on Rc [5.5, 8.5] GV.
- ❖ Demonstration of the reconstruction capability in time intervals of ~1 hour.

The HENSA++ spectrometer

- HENSA++ is the latest iteration of HENSA (**16 detectors**). During the last 2 years it has been under commissioning.
- Design with **optimized resolution**, overall in the high-energy region.
- Monitor the cosmic-ray neutron spectrum for space weather and ambient dosimetry research.

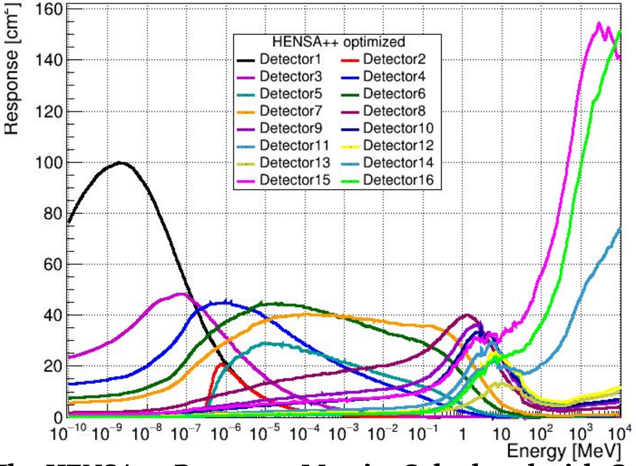

The HENSA++ Response Matrix. Calculated with Geant4.

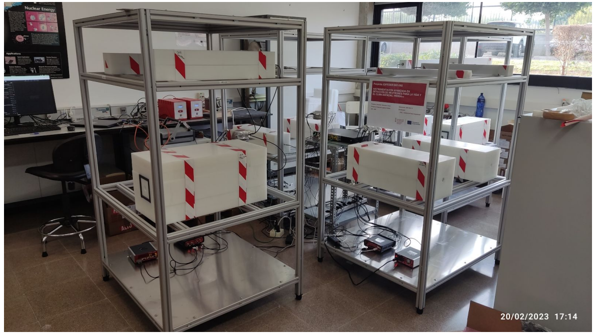

HENSA++ commissioning setup (IFIC Gamma & Neutron Lab)

HENSA++ first outdoors measurement (Zaragoza, Spain)

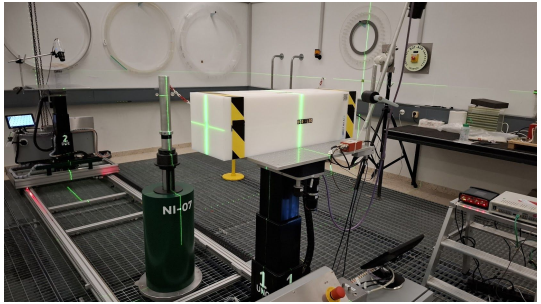

HENSA++ benchmarking exercise with AmBe neutron source (PSI, Switzerland)

Preliminary results of the commissioning phase

First Outdoors Cosmic-ray neutron measurements

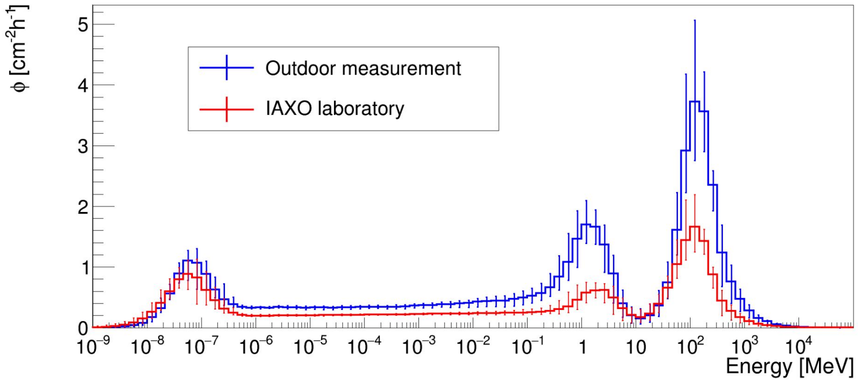

Reconstructed cosmic-ray neutron spectrum. Blue line: Outdoors, Red line: IAXO laboratory

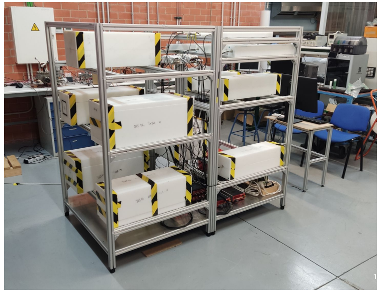

Detection of the May 2024 FD

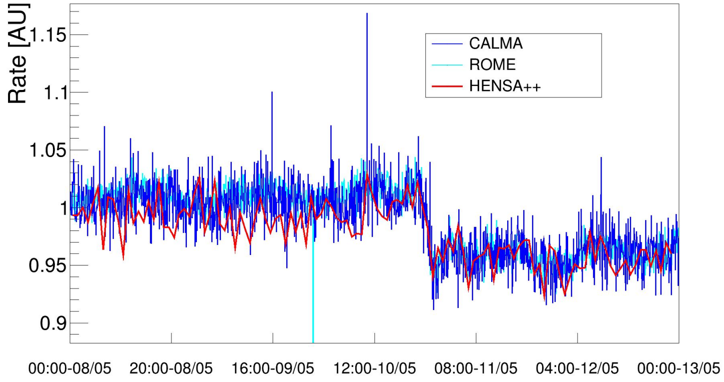

Temporal rate evolution of HENSA++ and the neutron monitor stations CALMA (6.95 GV) and ROME (6.25 GV) during the FD of May 2024.

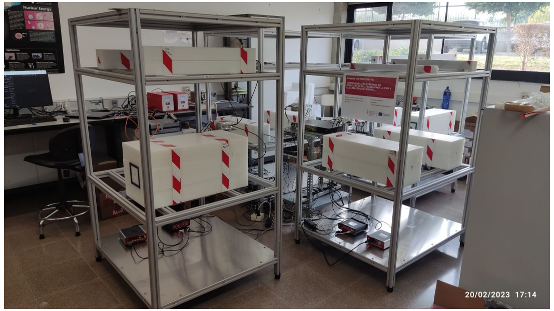

Final emplacement: Phase 0 commissioning

HENSA++ Space weather & Dosimetry

- We are commissioning a first reduced version of HENSA++ at the Observatorio Astrofísico de Javalambre in Spain (1957 masl, Rc = 7.07 GV) since 31/10/2024.
- This reduced version is composed of a low, an intermediate, and a high-energy detector.
- We are planning to install the full setup during this month (Phase 1).

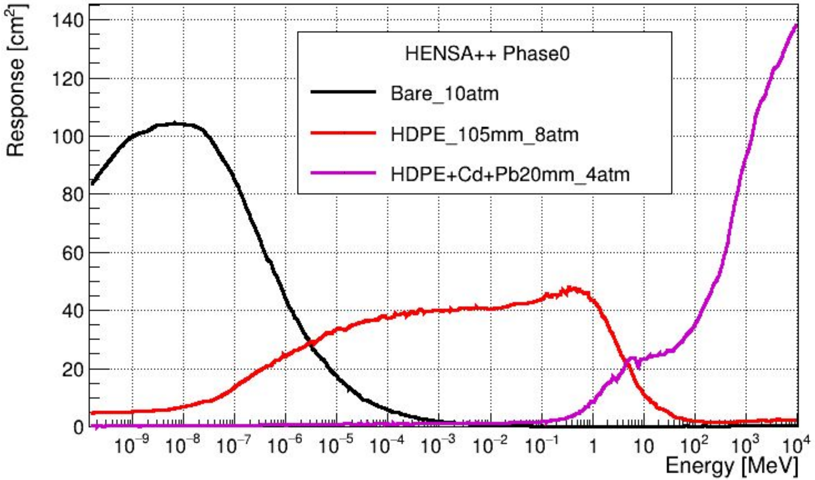

Recent Observation of a G4 Geomagnetic Solar Storm - 31/05/2025

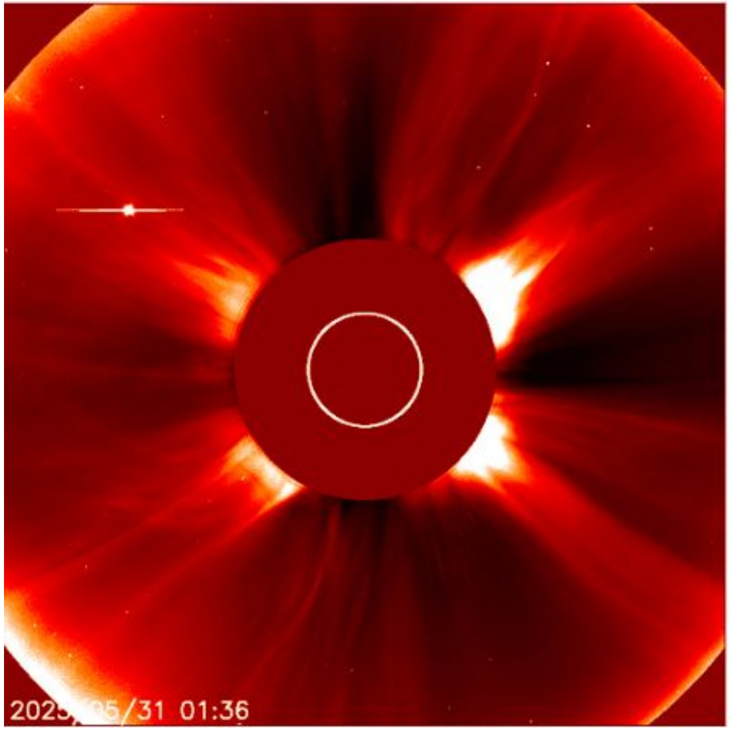

Image recorded by the NOAA LASCO C2 coronagraph from 31/05 to 01/06.

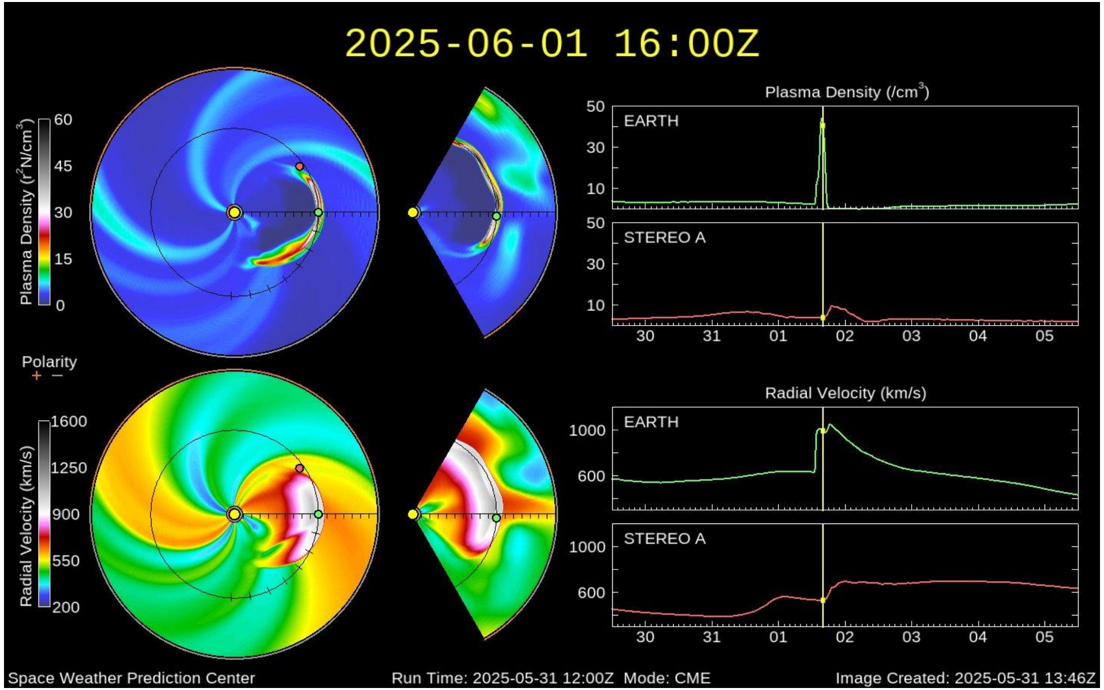

NOAA model prediction about the propagation of the CME.
https://www.ncei.noaa.gov/products/space-weather/partners/swpc-products-and-data

Observed Forbush Decrease on the Earth

- 15 mins timescale.
- Temporal evolution of the sum of the 3 channels.
- Same trend as the NMDB with only 3 detectors!

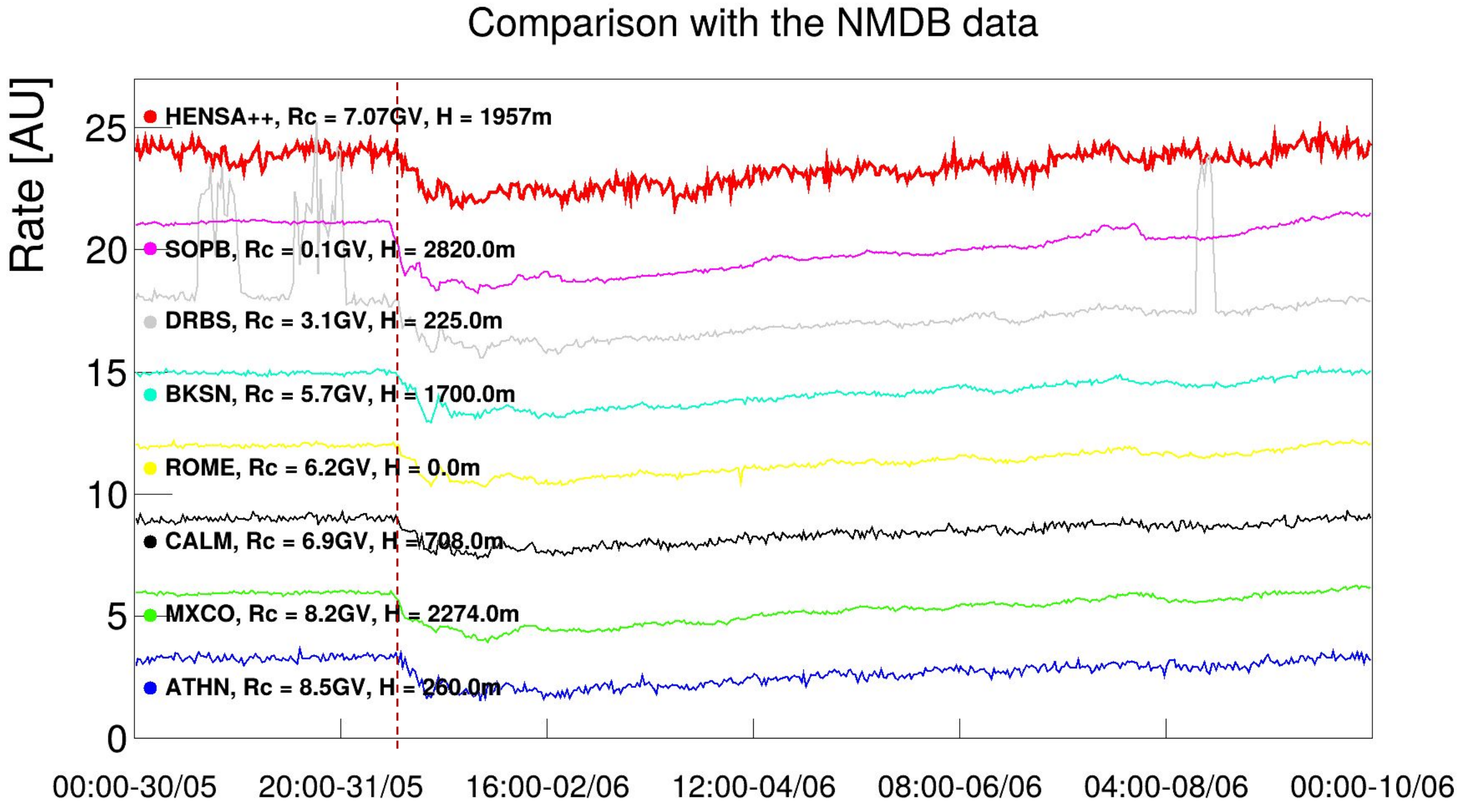

Comparison of each channel with satellite data

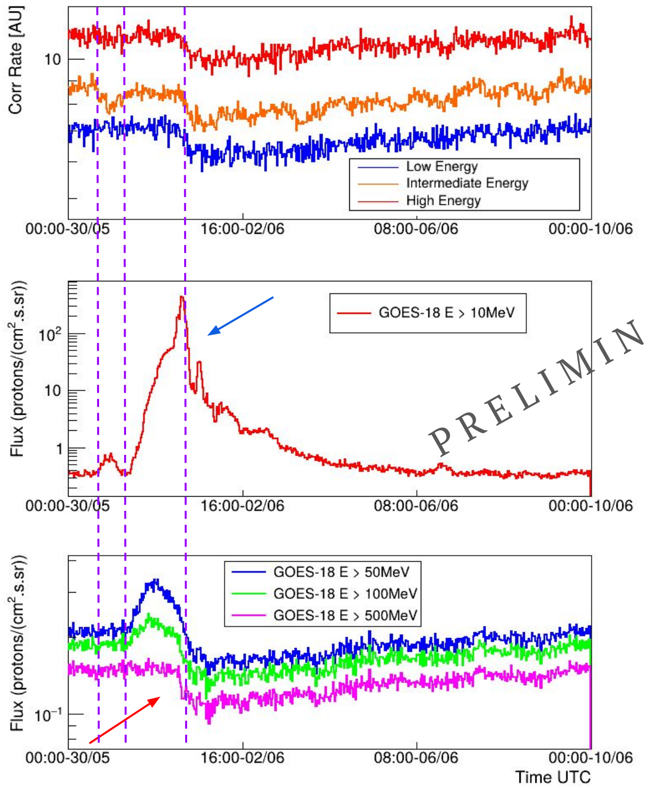

Temporal evolution of the 3 HENSA++ detectors placed at OAJ and the GOES-18 recorded proton flux

PRELIMINARY

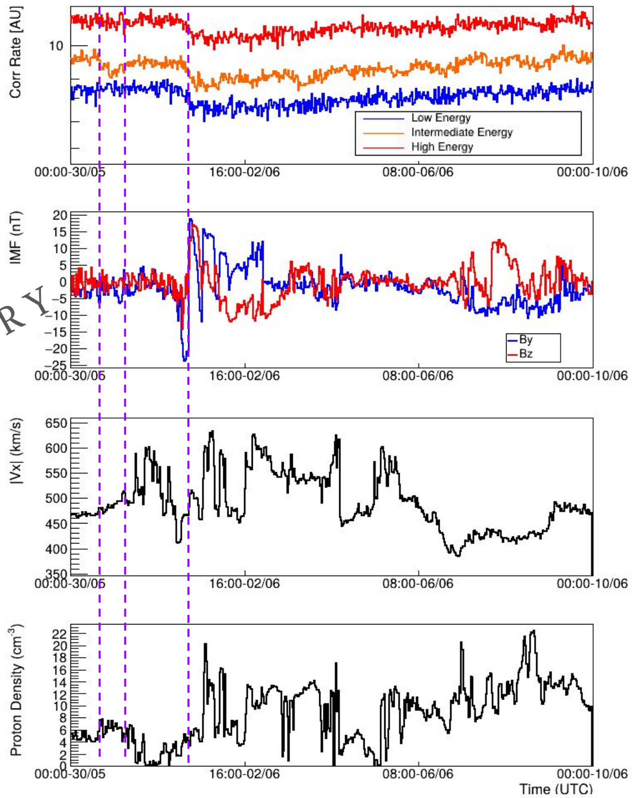

Temporal evolution of the 3 HENSA++ detectors placed at OAJ and the NOAA recorded magnetic field, proton density and velocity.

- Suddenly decrease on the high-energy proton component that produced this FD.
- Fast fluctuations on the IMF and the proton density and velocity profiles.
- Strange decrease of the intermediate channel before the FD (?).

Final remarks

- The HENSA project provides complementary spectral sensitivity to the NMDB, enhancing the analysis of primary cosmic-ray impacts on Earth.

- We have characterized the cosmic-ray neutron spectrum across a broad range of magnetic rigidities.

- The HENSA++ detector has been successfully commissioned in its final emplacement, showing consistency with NMDB measurements and effectively detecting recent solar events.

- We aim to collaborate with the Solar Physics community to better understand the influence of solar activity and high-intensity solar events on secondary radiation at ground level.

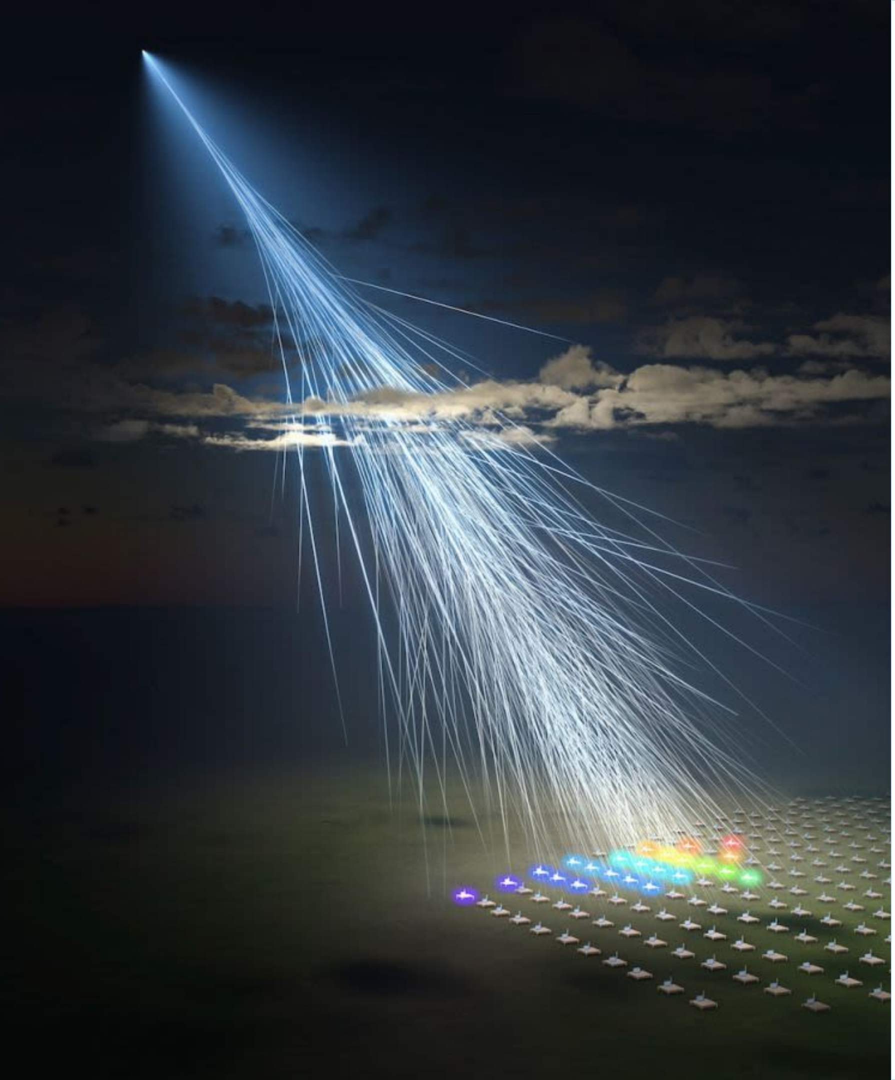

HENSA
High Efficiency Neutron Spectrometry Array

Thank you for your attention!

HENSA++
Space weather & Dosimetry

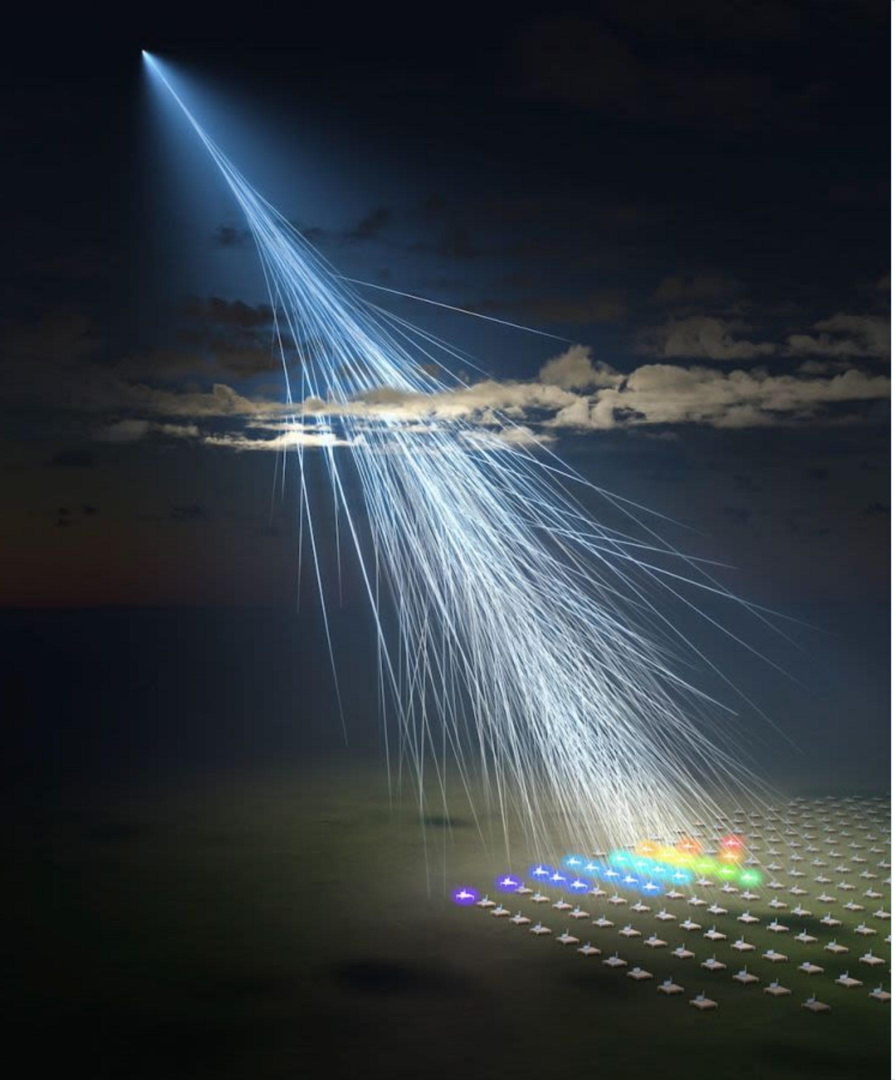

Backup

Solar modulation of the primary spectrum

Solar Minimum

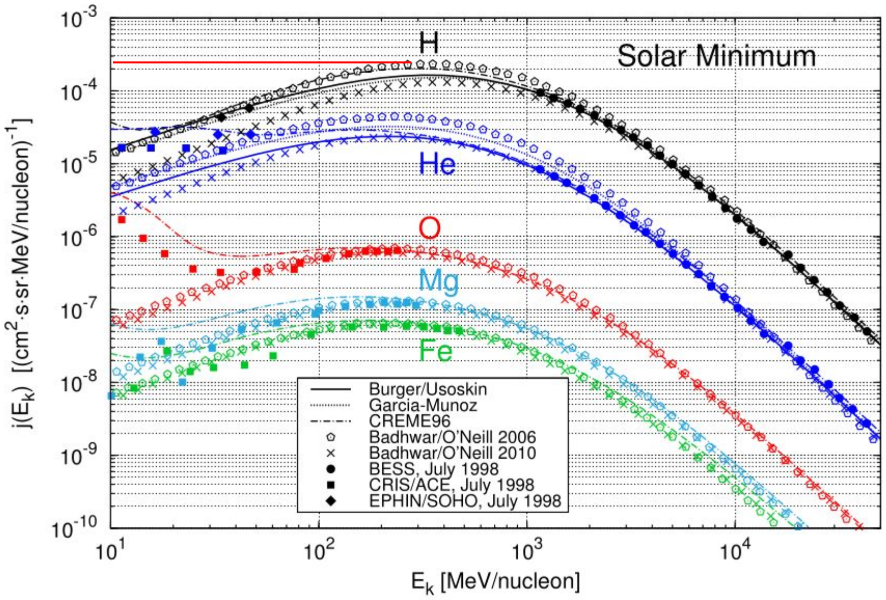

Solar Maximum

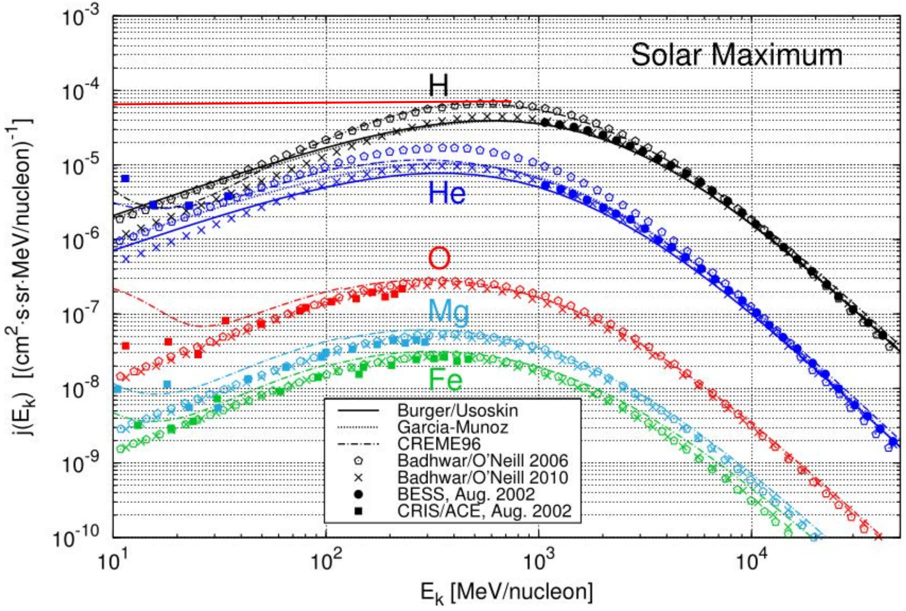

Differential particle intensities of primary galactic H, He, O, Mg, and Fe ions as a function of kinetic energy per nucleon measured near Earth during the BESS experiments (Sanuki et al., 2000; Haino et al., 2004), with the CRIS detector on-board ACE (Stone et al., 1998; Haino et al., 2004), and with EPHIN on-board SOHO (Müller-Mellin et al., 1995) in July 1998 (top panel), i.e. solar minimum, and Augus 2002 (bottom panel), i.e. solar maximum conditions. Experimental data are compared with predictions using models of Burger/Usoski (Burger et al., 2000; Usoskin et al., 2005), Garcia-Munoz (Garcia-Munoz et al., 1975), CREME96 (Tylka et al., 1997), and Bad-hwar/O'Neill (O'Neill, 2006, 2010). Pioch PhD Thesis (2012)

Behaviour of charged particles in the Earth magnetic field

The Earth magnetic field acts as a shielding against cosmic-rays

$$R = \frac{pc}{|q|} = \frac{pc}{Ze} = r_L |\vec{B}| c$$

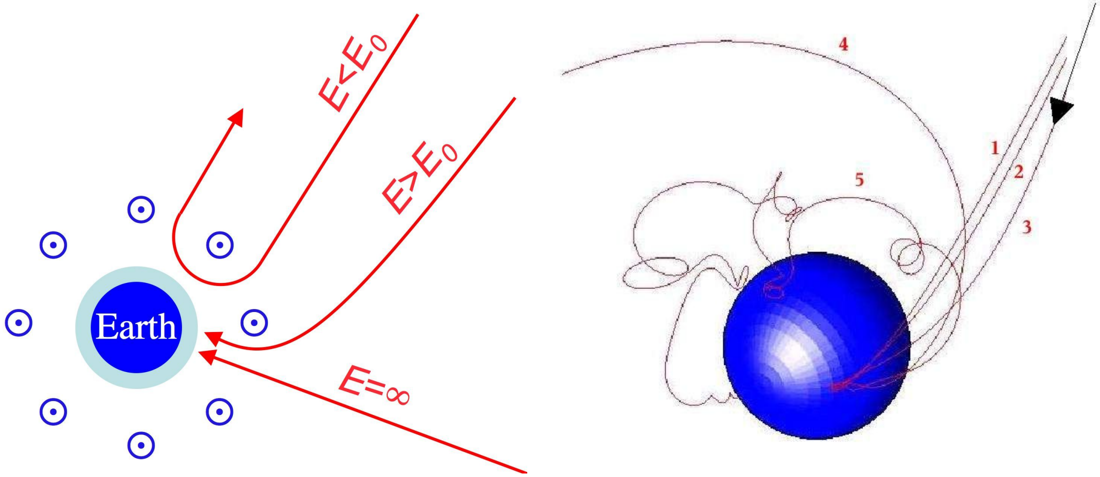

Trajectories of charged particles in the Earth magnetic field. From: https://www.nmdb.eu/public_outreach/es/03/

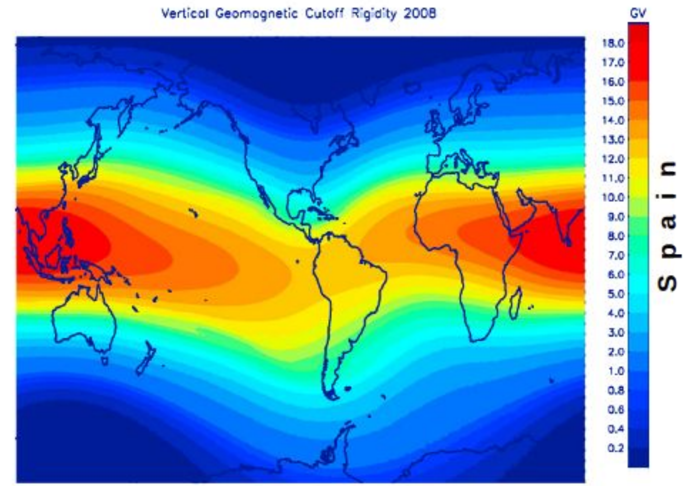

Figure 3. Global grid of vertical geomagnetic cutoff rigidities (GV) calculated from charged particle trajectory simulations in the IGRF field for 2008.

The origin of background neutrons

At surface level

Nuclear cascade reactions generated by primary cosmic-rays (p^+, He)

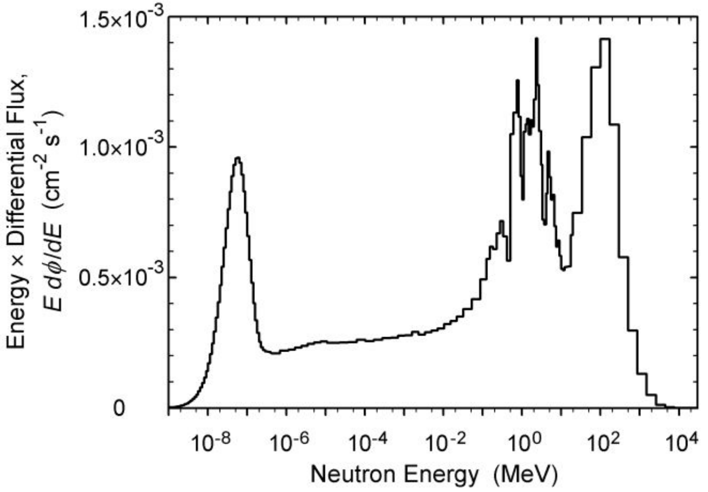

Measured cosmic-ray neutron spectrum on Yorktown Heights, NY. Gordon et al (2004), IEEE 51(6)

In underground laboratories

- (α, n) reactions on rocks
- Spontaneous Fission (U/Th)
- Neutrons induced by cosmic muons

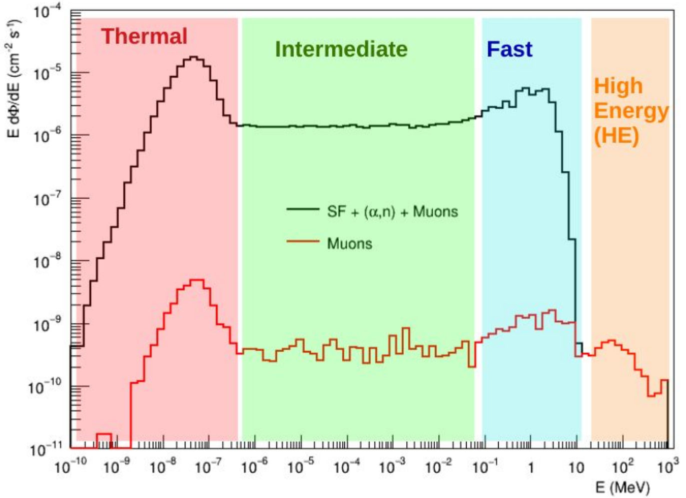

MC simulation for LSC Hall A (N. Mont-Geli, UPC)

HENSA setup: “active part”

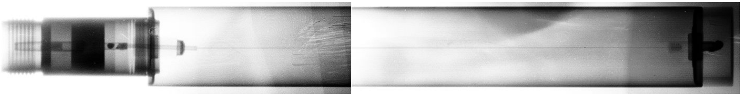

Detection reaction:

$$^{3}He + n \rightarrow {}^{3}H + p \qquad Q=0.764\ MeV$$

High Thermal cross section!!: **5330b**

Table 13-1. Neutron and gamma-ray interaction probabilities in typical gas proportional counters and scintillators

	Interaction Probability	
Thermal Detectors	Thermal Neutron	1-MeV Gamma Ray
^{3}He (2.5 cm diam, 4 atm)	0.77	0.0001
Ar (2.5 cm diam, 2 atm)	0.0	0.0005
BF_3 (5.0 cm diam, 0.66 atm)	0.29	0.0006
Al tube wall (0.8 mm)	0.0	0.014
	Interaction Probability	
Fast Detectors	1-MeV Neutron	1-MeV Gamma Ray
^{4}He (5.0 cm diam, 18 atm)	0.01	0.001
Al tube wall (0.8 mm)	0.0	0.014
Scintillator (5.0 cm thick)	0.78	0.26

*Extracted from Neutron Detectors, T. W. Crane and M. P. Baker

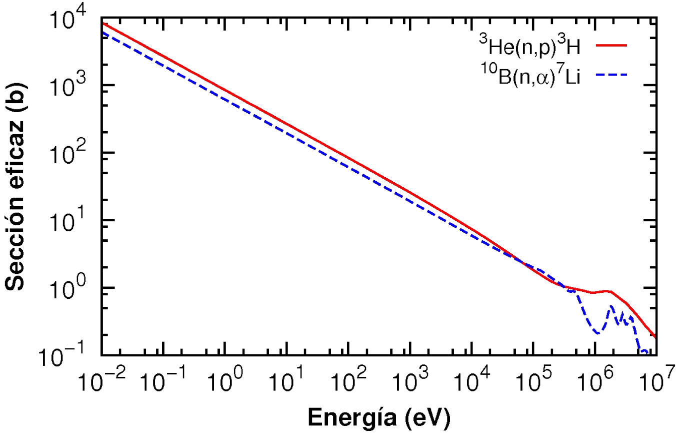

- These neutron counters are gaseous ionization detectors that use 3He as converting gas.
- Due to the high thermal capture cross section, 3He filled counters have a high neutron sensitivity.
- For non-thermal neutrons, the high efficiency can be exploited by using moderators.
- In addition, the low gamma-ray sensitivity makes these detectors very attractive for neutron spectroscopy (Bonner spheres).

HENSA comparison with BSS

Standard extended Bonner Spheres

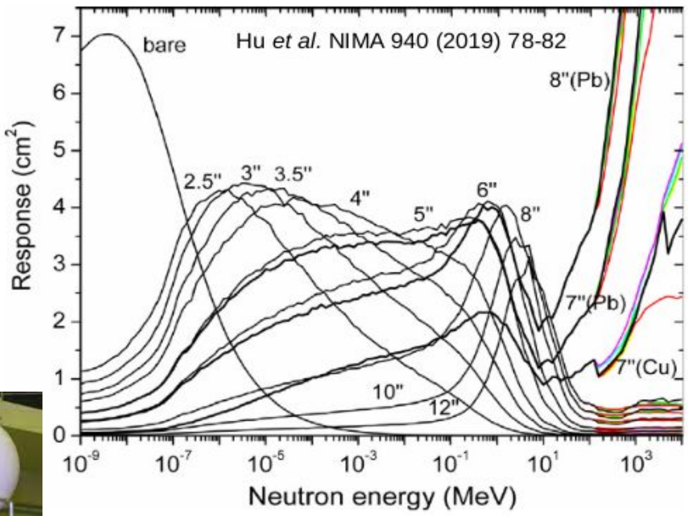

HENSA 2019 version

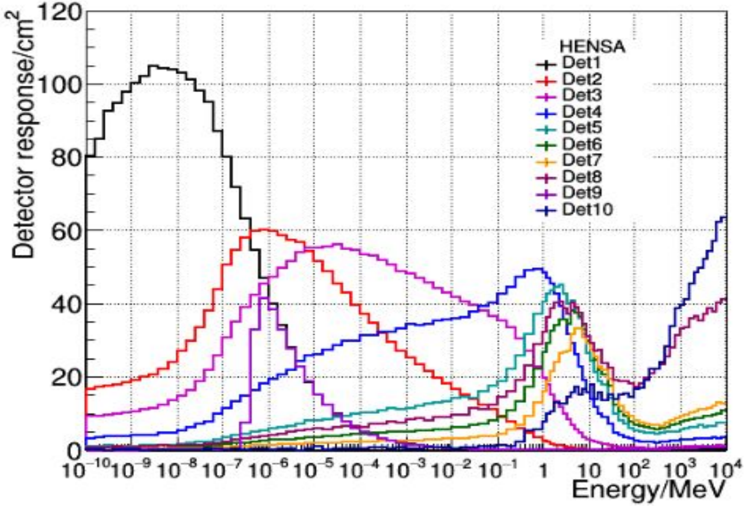

- ❖ HENSA neutron response is **5-15** times greater than standard BSS thanks to the increase in the detector active length
- ❖ The change in the topology is not a problem in isotropic fields

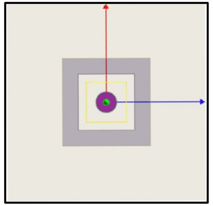

Optimization of HENSA++: Resolving power kernels

HENSA++ Space weather & Dosimetry

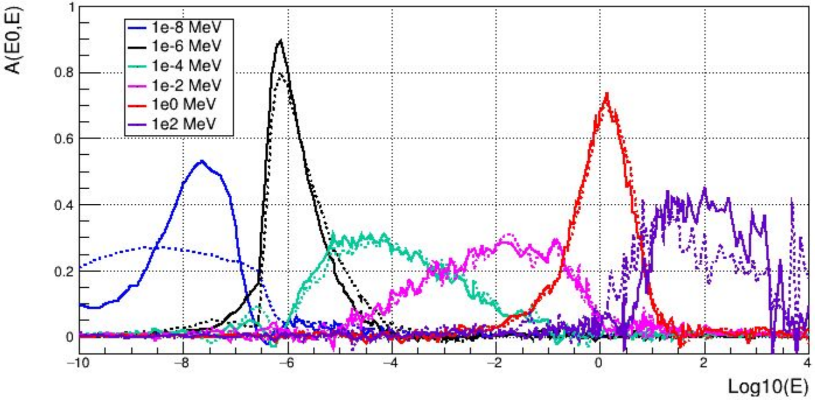

Dotted: Initial | Continuous: Optimized

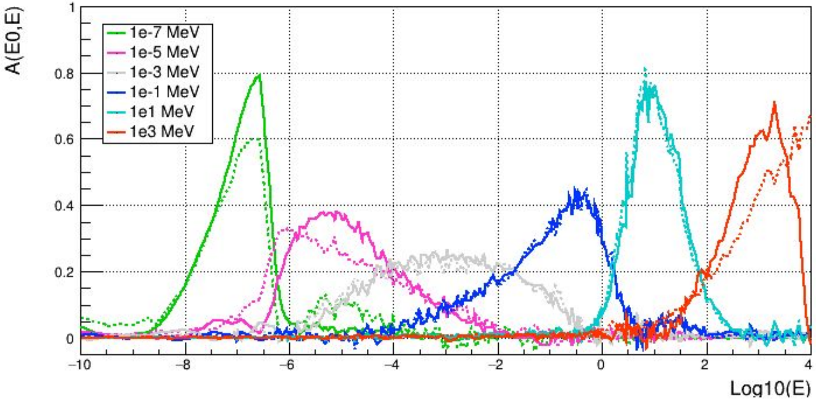

LogE	Mean(vInit)	Mean(vOpt)	SD(vOpt)/SD(vInit)-1
-8	-7.72	-7.69	-44.20%
-7	-6.76	-6.86	-51.11%
-6	-5.76	-5.89	-20.37%
-5	-4.93	-4.86	-24.11%
-4	-3.93	-3.98	-4.65%
-3	-3.00	-2.98	-8.27%
-2	-2.07	-2.08	-2.13%
-1	-1.12	-1.09	2.56%
0	-0.08	-0.09	-1.71%
1	0.91	0.94	-2.15%
2	1.43	1.72	-38.90%
3	2.71	2.73	-39.72%

ELSEVIER
Nuclear Instruments and Methods in Physics Research A 480 (2002) 690–695
NUCLEAR INSTRUMENTS & METHODS IN PHYSICS RESEARCH Section A
www.elsevier.com/locate/nima

Resolving power of a multisphere neutron spectrometer

Marcel Reginatto*

$$< \phi >_{E_0} = \int A(E_0, E)\phi(E)dE$$

Unfolding Parametric codes

- Parametric codes: Model the neutron spectrum based on the physics of neutron interactions (e.g., MITOM, FRUIT).
- They generate multiple spectra using Monte Carlo sampling and select the one that best fits the data by minimizing the chi-squared value.

$$\chi^2 = \frac{1}{n}\sum_{i=1}^{n}\left(\frac{C_i^{input} - C_i^{output}}{\sigma_i^{input}}\right)^2$$

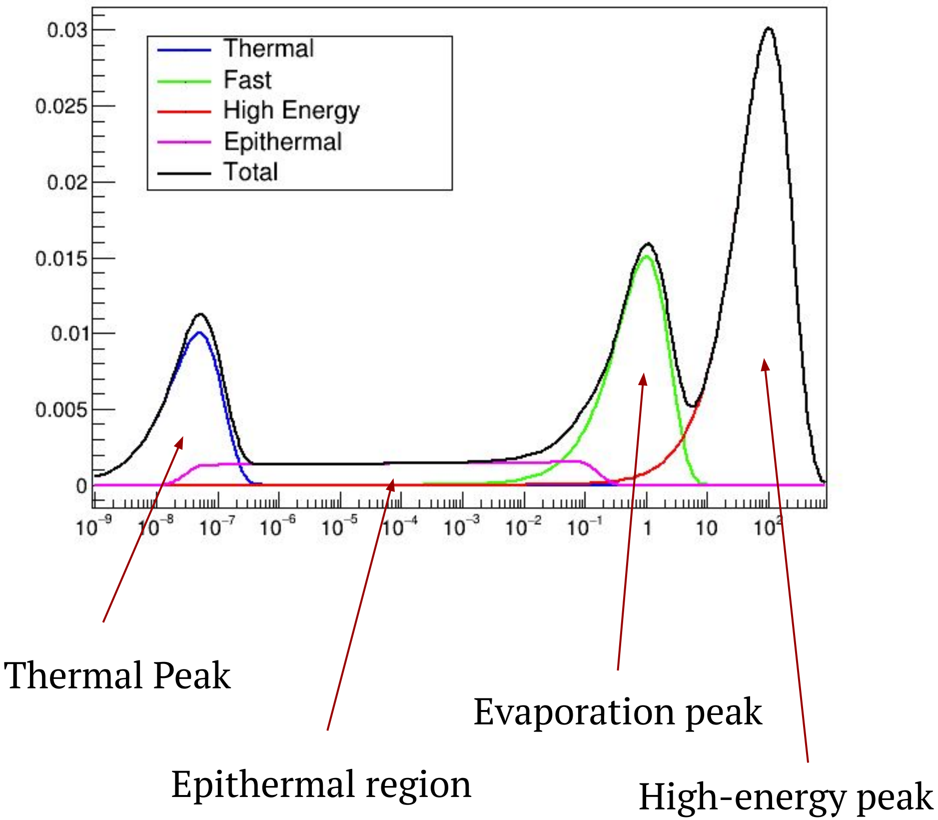

Unfolding Iterative codes

- Iterative codes: Employ some "a priori" spectrum and perturb it iteratively based on mathematical algorithms (eg. MAXED, GRAVEL, BAYES)
  - Entropy maximization (Information Theory)

$$\max:\ S[\mathbf{f}] - \frac{1}{\lambda}\chi^2[\mathbf{f}] \qquad S[\mathbf{f}] = -\sum_{i=1}^{n}\left(f_i \ln\frac{f_i}{h_i} - f_i + h_i\right)$$

  - Expectation maximization (Bayes Theorem)

$$\hat{f}_j = \frac{1}{\sum_{i=1}^{n} R_{ij}} \sum_{i=1}^{n} P(f_j|d_i)\hat{d}_i, \quad j = 1, \ldots, m$$

These codes iterate until some stopping criteria is reached. Usually, chi-squared:

$$\chi^2 = \frac{1}{n}\sum_{i=1}^{n}\left(\frac{C_i^{input} - C_i^{output}}{\sigma_i^{input}}\right)^2$$

$$\chi^2 \approx 1$$

Recent activities with HENSA++ at the Paul Scherrer Institute (PSI)

Intercomparison exercise BSS measurements (p-channel, Target M)

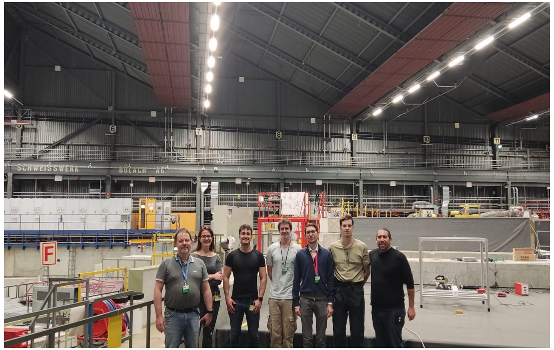

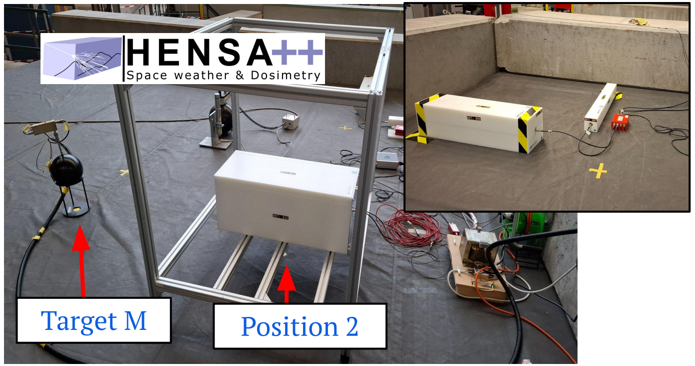

Benchmarking measurements with AmBe source (Calibration laboratory)

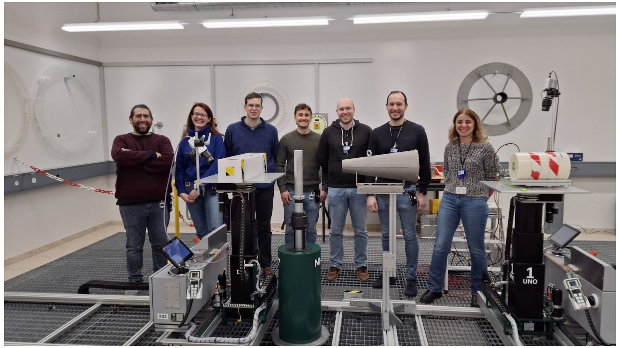

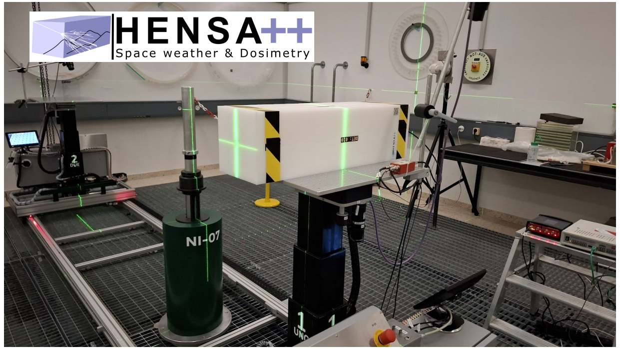

Applications: Underground (I)

HENSA
High Efficiency Neutron Spectrometry Array

HENSA at Felsenkeller, Germany (2020)

M Grieger et al (2020), Phys Rev D, 101, 123027

HENSA at LSC Hall A, Spain (2020)

SEA Orrigo et al (2022), Eur Phys Journal C, 82, 814

Applications: Underground (II)

HENSA
High Efficiency Neutron Spectrometry Array

HENSA at LSC Hall B, Spain (Since 2021)

N Mont-Geli et al (2023), Proceeding of Science 441, 312

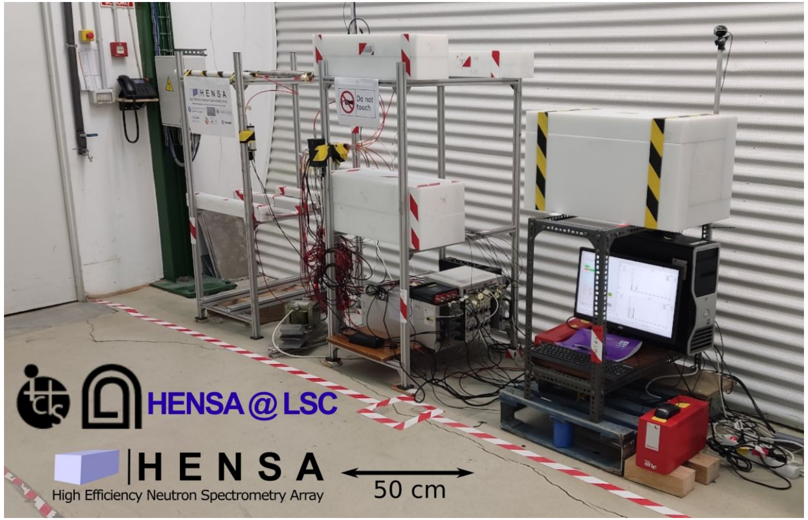

HENSA at LNGS, Gran Sasso, Italy (Since 2024)

Comparison of each channel with meteo data

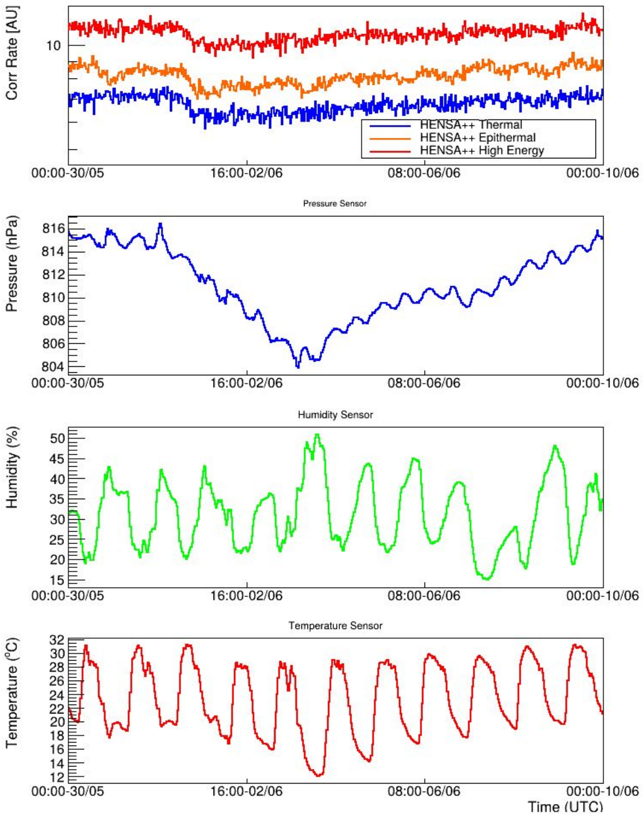

GSE coordinate system